International Journal of Scientific Research and Engineering Development-– Volume X Issue X, Year

Available at www.ijsred.com

RESEARCH ARTICLE OPEN ACCESS

AI-Driven Enhanced Lung Segmentation

W.A. Lahiru Randika[1], Jayanga Palihena[2]

[1](School of Artificial Intelligence, Nanjing University of Information Science and Technology, Nanjing
Email: lahirurandika@hotmail.com)

[2](School of Artificial Intelligence, Nanjing University of Information Science and Technology, Nanjing
Email: jayanga.sl@gmail.com)

----------**********----------

Abstract:

In the last decade, the usage of neural networks and deep learning methodologies has revolutionized medical image tasks, particularly in tasks such as image segmentation, classification, and segmentation, leading to significant advancements in diagnostic accuracy and treatment efficacy. Chest X-rays, a vital tool in medical imaging, play a key role in finding and understanding different chest problems, like lung diseases and heart issues. However, even though they're widely used, accurately and efficiently separating specific organs in chest X-rays remains a significant challenge for doctors because of the complicated structure of the body and different ways X-rays are taken. This study proposes a novel approach utilizing the U-Net architecture model for lung segmentation with unprecedented accuracy and robustness, aiming to address the longstanding challenges in medical image analysis.

In this research we have conducted numerous experiments, encompassing various optimization strategies such as Adam, RMSprop, and SGD, coupled with observed fine-tuning of hyperparameters. These efforts result in the development of a state-of-the-art model architecture, showcasing remarkable performance metrics with training and validation accuracies consistently surpassing the 96% threshold. This exceptional level of accuracy, coupled with the utilization of the Dice coefficient as the loss function, shows how effective and reliable our approach is at outlining lung borders with exceptional precision. Additionally, by using a combined dataset of over 900 chest X-rays carefully labelled by doctors, we made sure our model is robust and generalizable, which makes it more useful in real-world situations.

The findings of this research contain the efficacy of the proposed model in lung segmentation that offers improved model performance and enhanced generalization capabilities. By addressing the challenges of overfitting while maintaining model efficiency, this study contributes to the advancement of medical image segmentation methodologies, facilitating more accurate and efficient diagnosis and treatment planning for thoracic abnormalities.

Keywords — **Lung Segmentation, Deep Learning, U-Net, Medical Imaging, Automated Segmentation.**

----------**********----------

I. INTRODUCTION

Lung segmentation from medical images plays a pivotal role in computer-aided diagnosis and treatment planning for various pulmonary diseases. Accurate delineation of lung regions enables clinicians to analyze lung morphology, detect abnormalities, and monitor disease progression. Traditional methods for lung segmentation often rely on handcrafted features and heuristic algorithms, which are limited in their ability to handle complex image structures and variations in image quality. In recent years, deep learning techniques have emerged as a powerful tool for medical image analysis,

offering superior performance in various segmentation tasks.

In this article, we present a novel approach to lung segmentation using deep learning, specifically leveraging the U-Net architecture. Before delving into our methodology, we provide an overview of existing lung segmentation methods and highlight the challenges faced by traditional approaches. Saood and Hatem introduced a U-Net-based method for lung segmentation in 2021 [1] achieving promising results in terms of accuracy and Dice coefficient. Similarly, Xavier Annie proposed a U-Net model for lung segmentation in 2023 [2], although with lower performance compared to other methods. Rudiansyah and other researchers presented a U-Net-based approach with competitive performance in terms of accuracy and Dice coefficient [3].

Motivated by the limitations of existing methods and the potential of deep learning, we developed a novel methodology for lung segmentation using the U-Net architecture. Our approach involves preprocessing of input data, model training using the U-Net architecture, and evaluation of segmentation performance using standard metrics. To optimize model performance, we experimented with different optimizers and learning rates, as well as hyperparameter tuning techniques. Our experimental results demonstrate the effectiveness of our approach, with superior accuracy and segmentation quality compared to state-of-the-art methods [4].

Through this article, we aim to contribute to the advancement of medical image analysis and the development of automated segmentation methods for lung disease diagnosis and treatment planning. By providing a detailed description of our methodology and experimental results, we hope to inspire further research in this field and facilitate the adoption of deep learning techniques for lung segmentation in clinical practice.

II. LITERATURE REVIEW

The literature surrounding lung segmentation from medical images encompasses a diverse array of methodologies, ranging from traditional techniques to cutting-edge deep learning approaches. Lung segmentation plays a pivotal role in computer-aided diagnosis and treatment planning for pulmonary diseases, necessitating the exploration of robust and efficient segmentation methods [5]. This review aims to provide a comprehensive overview of existing approaches for lung segmentation, shedding light on both conventional methodologies and recent advancements in deep learning-based techniques.

Traditional methods for lung segmentation have historically relied on heuristic algorithms and image processing techniques to delineate lung regions from medical images. These methods often involve thresholding, region growing, active contours, and morphological operations to extract relevant anatomical structures. While traditional approaches have demonstrated effectiveness in certain scenarios, they are inherently limited by their reliance on handcrafted features and assumptions about image characteristics. For instance, Saood and Hatem (2021) [1] proposed a lung segmentation method based on thresholding and morphological operations, showcasing the utility of traditional techniques in medical image analysis.

In recent years, deep learning-based approaches have emerged as a paradigm shift in medical image segmentation, offering remarkable performance improvements over traditional methods. Among the pioneering architectures in this domain is U-Net, introduced by Ronneberger [6], which revolutionized medical image segmentation tasks with its encoder-decoder architecture and skip connections. U-Net has since become a cornerstone in medical image analysis, with numerous studies leveraging its architecture for various segmentation tasks. For instance, [2] employed a U-Net model for lung segmentation, demonstrating the efficacy of deep learning in accurately delineating lung regions from medical images. [3] also utilized a U-Net-based approach for lung segmentation, achieving high accuracy and Dice coefficient values.

In light of the advancements and limitations highlighted in the literature review, the objective of this research is to develop a U-Net-based model tailored for accurate and efficient lung segmentation

from medical images. By leveraging the capabilities of deep learning and specifically the U-Net architecture, this study aims to address the challenges posed by traditional segmentation methods, such as manual feature engineering and limited adaptability to diverse image characteristics [7]. The proposed model seeks to enhance the accuracy, robustness, and scalability of lung segmentation, ultimately contributing to the advancement of computer-aided diagnosis and treatment planning for pulmonary diseases [8].

III. METHODOLOGY

The methodology adopted for this research encompasses several key components, including the utilization of the U-Net architecture, data pre-processing techniques, and the training process tailored to optimize model performance.

The U-Net architecture, initially proposed by Ronneberger [6], has garnered significant attention in medical image segmentation tasks due to its inherent ability to capture spatial dependencies and generate accurate segmentation masks. Its unique design, characterized by a contracting path followed by an expansive path, facilitates the extraction of intricate features while preserving spatial information, making it particularly suitable for segmentation tasks with complex anatomical structures.

A. Dataset Preparing & Data Preprocessing

Dataset preparation is a crucial step in training and evaluating deep learning models for lung segmentation, and data preprocessing plays a vital role in enhancing the quality and usability of the dataset for training deep learning models. There are several datasets available for lung segmentation such as LUNA16, VESSEL12, CRPF, JSRT, CXR-14, CheXpert, Montgomery Country CXR, Shenzhen CXR database. After conducting a thorough research in the literature review we have selected Kaggle CXR dataset for our research. This dataset consisted with both Montogomery Country CXR and Shenzhen CXR datasets. We considered several factors before selecting the dataset such as dataset scale, diversity, annotated ground truth, community contribution, validation by healthcare professionals and publicly accessibility.

1) ***Data Loading and Preprocessing:*** The dataset consists of CXR images and corresponding masks. The images are loaded and resized to a predefined shape, typically (256, 256) pixels and the pixel values of the images are normalized to the range [0,1] to facilitate model training.

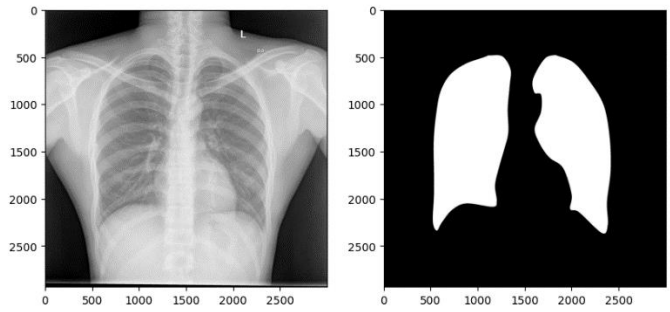

Fig. 1 Raw CXR and Mask

The above figure 1 displays the original CXR image and its corresponding mask image. This provides a visual representation of the raw data used in the dataset.

2) ***Train-Test Split:*** Once the images and masks are loaded and pre-processed the dataset is split into training and testing sets. In the initial training we will split 80% for training and 20% for validating as the standard metrics, then we will perform experiments increasing and decreasing validating set and observe the results.

3) ***Reshaping:*** Before feeding the data into the neural network model, the images and masks are reshaped to conform to the model's input requirements.

4) ***Normalization:*** Following reshaping, the pixel values of the images and masks are normalized to the range [0,1] to standardize the pixel intensity values across the dataset and helps in stabilizing the training process.

5) ***Data Augmentation:*** To increase the diversity and robustness of the training data augmentation techniques are applied. Various transformations such as rotation, translation, shearing, zooming, flipping and brightness adjustment are performed on the images to prevent overfitting and improve the model's generalization ability [9].

B. Proposed Model

The proposed model is based on U-Net model and the primary objective is to accurately delineate lung regions from CXR images, facilitating subsequent analysis and diagnosis.

predefined threshold for a certain number of epochs,

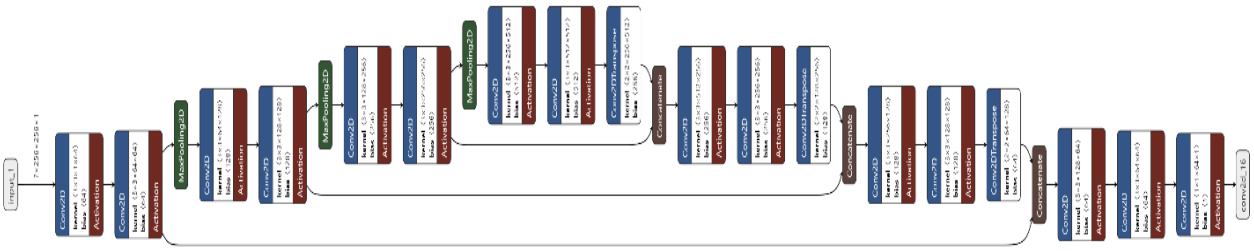

Fig. 2 Proposed Model Architecture

The proposed model featuring an encoder-decoder structure with skip connections. The input layer accepts grayscale images of size 256x256 pixels and it consist of four blocks with two convolutional layers each, followed by max-pooling for down-sampling. Similarly, the decoder comprises four blocks with two convolutional layers each, followed by transpose convolutions for up-sampling. Skip connections concatenate feature maps from corresponding encoder blocks to aid in precise localization. The final layer is a convolutional layer with a sigmoid function, producing a binary mask indicating lung regions in the input image. Above figure 2 provides an overview of model's architecture.

C. Learning Rate

A learning rate scheduler function was defined to adjust the learning rate based on the epoch. Initially set to a base learning rate, then scheduler reduces the learning rate by a factor of 0.1 after 10 epochs and by another factor of 0.1 after 20 epochs.

Plateau learning rate scheduling, also known as ReduceLROnPlateau, is a technique used in training deep learning models to dynamically adjust the learning rate based on the model's performance during training. The primary objective of plateau scheduling is to automatically reduce the learning rate when the model's performance stagnates or plateaus, thereby facilitating convergence to a better solution [10].

The idea behind plateau scheduling is to monitor a specified metric, such as validation loss or accuracy, over a certain number of epochs. If the metric does not show improvement beyond a the learning rate is reduced by a factor, allowing the optimizer to escape from local minima or plateaus [11]

The plateau learning rate scheduling strategy can be mathematically represented as: if metric does not improve f or patience epochs

$$new_{lr} = lr \times factor \qquad (1)$$

Where metric is the monitored performance metric (e.g., validation loss). Patience is the number of epochs with no improvement after which learning rate will be reduced, lr is the current learning rate. And factor is the factor by which the learning rate will be reduced (typically a value between 0 and 1).

The reduction in learning rate helps the optimizer to take smaller steps in the parameter space, potentially escaping from local minima and finding a better solution.

Plateau learning rate scheduling is particularly useful in scenarios where the loss landscape is non-convex and contains numerous local minima. By dynamically adjusting the learning rate based on the model's performance, plateau scheduling allows for more efficient optimization and can lead to better generalization on unseen data.

D. Implementing Different Optimizers

We experimented with three popular optimizers: Adam, RMSProp and SGD to explore the impact of different optimizers [12].

1) Adam

Adam is an adaptive learning rate optimization algorithm that combines the advantages of two other popular optimization techniques: RMSProp and momentum. It maintains separate learning rates for

each parameter and updates them based on the estimates of the first and second moments of the gradients [13].

Below are the equations related to Adam optimizer:

Momentum Update

$$m_t = \beta_1 m_{t-1} + (1-\beta_1) g_t \quad (2)$$

Here, m_t represents the exponentially decaying average of past gradients, β_1 is the exponential decay rate for the first moment estimate, g_t represents the current gradient, and t denotes the current time step.

Scaling of gradients update

$$v_t = \beta_2 v_{t-1} + (1-\beta_2) g_t^2 \quad (3)$$

Here, v_t represents the exponentially decaying average of past squared gradients, β_2 is the exponential decay rate for the second moment estimate, and g_t^2 represents the element-wise square of the current gradient.

Bias Correction

$$\widehat{m_t} = \frac{m_t}{1-\beta_1^t} \quad (4)$$

$$\widehat{v_t} = \frac{v_t}{1-\beta_2^t} \quad (5)$$

These equations perform bias correction to account for the initialization of m_t and v_t as zero vectors.

Parameter Update

$$\theta_{t+1} = \theta_t - \frac{\alpha}{\sqrt{\widehat{v_t}}+\epsilon}\widehat{m_t} \quad (6)$$

Here, θ_t represents the model parameters, α is the learning rate, ϵ is a small value to prevent division by zero, and $\widehat{m_t}$ and $\widehat{v_t}$ are the bias-corrected estimates of the first and second moments of the gradients, respectively [10].

Adam is widely used in deep learning applications due to its effectiveness in training neural networks and its ability to handle noisy gradients and sparse gradients. It automatically adapts the learning rate for each parameter, making it well-suited for a wide range of optimization problems.

2) RMSProp

RMSProp is an adaptive learning rate optimization algorithm that adjusts the learning rates of individual parameters based on the magnitudes of their gradients. It helps to overcome the vanishing or exploding gradient problem by scaling the learning rates differently for each parameter [12].

The RMSProp algorithm calculates a decaying average of the squared gradients for each parameter and uses this to normalize the learning rate. The parameter update rule is given by:

$$\theta_{t+1} = \theta_t - \frac{\alpha}{\sqrt{v_t}+\epsilon} g_t \quad (7)$$

Where θ_t is the parameter at time step t, α is the learning rate, v_t is the exponentially decaying average of the squared gradients, g_t is the current gradient, and ϵ is a small value added to the denominator for numerical stability.

The v_t term is calculated using the following equation:

$$v_t = \beta v_{t-1} + (1-\beta) g_2^t \quad (8)$$

Where β is a decay rate hyperparameter that controls the exponential decay of the moving average.

RMSProp is particularly effective in dealing with non-stationary environments and problems with sparse gradients. It adapts the learning rates of individual parameters based on their past gradients, which helps to improve convergence and stability during training [12]

3) SGD

Stochastic Gradient Descent is a classic optimization algorithm used for minimizing the loss function during training of machine learning models. In SGD, the parameters are updated in the opposite direction of the gradient of the loss function with respect to the parameters. It updates the parameters using the formula:

$$\theta_{t+1} = \theta_t - \alpha . \nabla J(\theta_t) \quad (9)$$

Where θ_t is the parameter vector at time step t, α is the learning rate, $J(\theta_t)$ is the loss function, and $\nabla J(\theta_t)$ is the gradient of the loss function with respect to the parameters [2].

E. Hyperparameter Tuning

We performed a grid search to find the optimal learning rates for each optimizer. The grid search parameters included different learning rates for Adam, RMSProp and SGD optimizers. Then we experimented with each optimizer by setting the learning rate to the values obtained from the grid search [12]. We employed hyperparameter tuning to further optimize our model. We defined a function to build our model with customizable hyperparameters, such as the number of filters in the convolutional layers. Random search was used to search the hyperparameter space and identify the best set of hyperparameters for the model. Model building function accepts hyperparameters as inputs and returns a compiled model ready for training.

Finally, we train the model using optimized hyperparameters for each optimizer.

F. Evaluation Metrics

We first analyze the training and validation losses to asses the model's convergence and generalization ability. The binary cross-entropy loss is plotted over epochs for both training and validation datasets.

Dice Coefficient is a common metric used to evaluate the performance of image segmentation models. It measures the overlap between the predicted and ground truth segmentation masks, providing a measure of segmentation accuracy[14]. We compute and plot Dice Coefficient over epochs for both training and validation datasets [15].

IV. EXPERIMENTS AND RESULTS

In this section, we delve into the experimental setup, training procedures, optimization strategies, and evaluation results of segmentation framework. Upon training our model with each optimizer for 20 epochs, we observed notable differences in their convergence behaviour and final performance metrics.

TABLE I
TRAINING RESULTS AND ANALYSIS OF OPTIMIZERS

Optimizer	Epochs	Loss	Dice Coefficient	Accuracy
Adam	10	0.0778	0.9189	0.9721
	20	0.0553	0.9367	0.9785
RMSProp	10	3.9224	0.2481	0.7450
	20	3.7224	0.4384	0.7450
SGD	10	0.5525	0.2690	0.7450
	20	0.5302	0.2970	0.7750

TABLE III
VALIDATION RESULTS AND ANALYSIS OF OPTIMIZERS

Optimizer	Epochs	Loss	Dice Coefficient	Accuracy
Adam	10	0.0757	0.9180	0.9719
	20	0.0574	0.9344	0.9779
RMSProp	10	3.8723	0.3966	0.7483
	20	3.8723	0.3964	0.7483
SGD	10	0.5455	0.2665	0.7483
	20	0.5274	0.2927	0.7786

Based on the results of our experiments, Adam emerged as the most suitable optimizer for our lung segmentation task. Its adaptive learning rate and momentum parameters enabled efficient exploration of the optimization landscape, leading to faster convergence and superior performance compared to RMSProp and SGD.

After conducting multiple trials with different hyperparameter configurations, we identified the best set of hyperparameters for each optimizer. Notably, the optimized hyperparameters resulted in a significant improvement in model performance.

V. EVALUATION RESULTS

After completing the final training using Adam optimizer and tuned hyperparameters for 40 epochs, we evaluated its performance on both the training and validation datasets. Below table 3 and table 4 summarizes the key metrics.

TABLE IIII
TRAINING EVALUATION RESULTS

Epochs	Loss	Dice Coef	Accuracy
1	0.5567	0.2887	0.7322
5	0.1690	0.8078	0.9361
10	0.0847	0.9084	0.9687
15	0.0632	0.9300	0.9758
20	0.0547	0.9386	0.9789
25	0.0519	0.9402	0.9794
30	0.0472	0.9466	0.9810
35	0.0469	0.9459	0.9821
40	0.0414	0.9522	0.9891

TABLE IV
EVALUATION RESULTS

Epochs	Loss	Dice Coef	Accuracy
1	0.4660	0.3327	0.7483
5	0.1434	0.8275	0.9470
10	0.0830	0.9096	0.9687
15	0.0593	0.9341	0.9769
20	0.0607	0.9277	0.9774
25	0.0529	0.9435	0.9798
30	0.0508	0.9475	0.9805
35	0.0496	0.9486	0.9812
40	0.0484	0.9493	0.9879

The evaluation results in above table 4 demonstrate the efficacy of trained model with progressively improving performance metrics across training epochs. The model achieved high accuracy and segmentation quality, laying the groundwork for its deployment in clinical settings for automated lung region delineation tasks. To graphically illustrate the model's performance, we have used Tensorboard to visualize the results and monitor the performance.

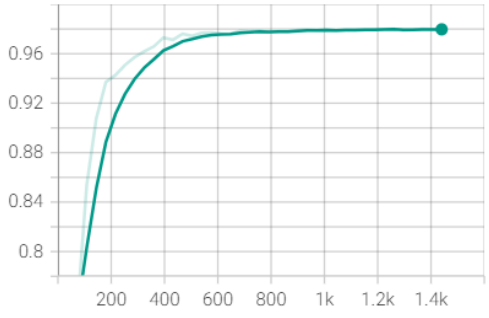

Fig. 3 Evaluation Binary Accuracy vs. Iterations

In above figure 3 the line represts the binary accuracy values computed during the evaluation of the model on the validation dataset.

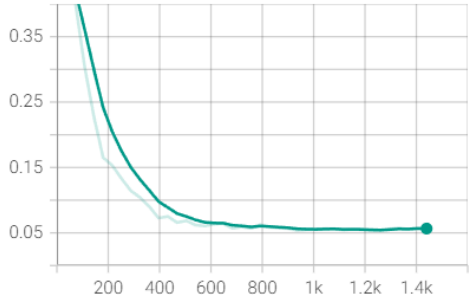

Fig. 4 Evaluation Loss vs. Iterations

Above figure 4 indicates the loss incurred by the model during evaluation on the validation dataset across iterations.

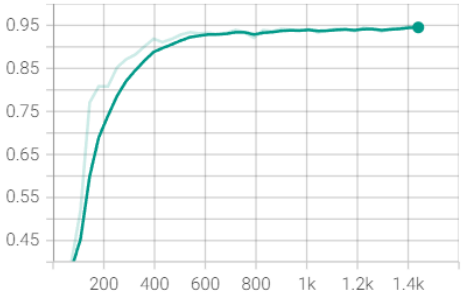

Fig. 5 Evaluation Dice Coef vs. Iterations

Above figure 5 presents Dice Coefficient of the model evaluated on the validation dataset through epochs. Dice Coefficient in table 4 measures the agreement between the predicted segmentation and the ground truth, with values ranging from 0 to 1.

The evaluation results presenting a significant improvement in the model's performance metrics over the course of training from epoch 1 to 40. At epoch 1 as in above figures (figure 3,4,5) and table 4, the model exhibited a relatively higher loss of 0.5366 and a lower Dice Coefficient of 0.2978 on the training dataset. The binary accuracy which measures the proportion of correctly classified pixels, stood at 0.7446. On the validation dataset, the model achieved a slightly lower loss of 0.4520 with a Dice

Coefficient of 0.3575 and a binary accuracy of 0.7504.

In table 3 and table 4 comparison, by epoch 40 the model demonstrated remarkable progress, achieving a significantly reduced loss of 0.0414, indicating improved convergence and effectiveness in capturing the underlying patterns in the data. The Dice Coefficient surged to 0.9522 indicating a substantial enhancement in the model's ability to accurately delineate lung regions. Moreover, the binary accuracy surged to 0.9831, highlighting the model's enhanced capability in correctly classifying pixels.

On the validation dataset, the model continued to display impressive performance, with a loss of 0.0566 and a dice coefficient of 0.9464, indicating strong segmentation quality and accuracy. The binary accuracy on the validation dataset remained high at 0.9839 showing the model's robustness and generalization ability.

Fig. 6 Predicted Mask vs. Mask I

Fig. 7 Predicted Mask vs. Mask II

Above both figure 6 and figure 7 demonstrate the model's ability to accurately segment lung regions, as evidenced by the close alignment between the predicted and real masks in the overlay. These figures serve to visually validate the effectiveness of the trained lung segmentation model, highlighting its potential for clinical applications in automated lung region delineation tasks.

Overall, the evaluation results demonstrate the effectiveness and robustness of the trained model, showcasing its potential capabilities in clinical applications for automated detection and analysis of lung abnormalities.

VI. COMPARISION WITH EXISTING WORK

To review the performance of proposed model, we conducted a comparative analysis with existing research efforts in the field.

TABLE V
COMPARISON WITH EXISTING METHODS

No	*Reference*	*Method Name*	*Accuracy*	*Dice Coef*
1	**Our Model**	**U-Net**	**0.9879**	**0.9466**
2	[1]	U-Net	0.948	0.733
3	[1]	SegNet	0.956	0.749
4	[2]	U-Net	0.91	0.4273
5	[3]	U-Net	0.9624	94.44
6	[16]	NASNet-Large-Decoder Net	-N/A	0.92
7	[17]	SMR-UNet	-N/A	0.9187
8	[18]	WI-U-Net++	0.9875	0.9342
9	[4]	U-Net	0.9387	0.9187
10	[19]	U-Net	0.9147	-N/A

Our U-Net based model achieved an accuracy of 98.79% and a Dice Coefficient of 94.66%. Comparative analysis with existing methods revealed that our model outperformed several approaches as shown in table 5. Our proposed model showcases its potential for accurate and precise lung segmentation, thereby contributing to advancements in medical image analysis and diagnosis.

VII. CONCLUSION

In conclusion, our research represents a significant stride forward in the realm of medical image analysis, particularly in the critical area of lung segmentation from chest CXR images. By harnessing the capabilities of deep learning and integrating novel architectural enhancements into the U-Net architecture, we have successfully developed a highly accurate and robust segmentation model.

Our findings highlight the potential of our proposed model to revolutionize clinical practice by enabling more precise and efficient interpretation of radiological images. The model's ability to accurately delineate lung regions, even in the

presence of diverse image qualities, noise levels, and pathological variations, holds immense promise for improving diagnostic accuracy and treatment planning in respiratory medicine.

However, it's important to acknowledge the inherent challenges and limitations associated with our research. While our model achieves impressive performance across various datasets, there remains room for further refinement and optimization. Future endeavors should focus on expanding the dataset, incorporating additional clinical annotations, and conducting rigorous validation studies in diverse clinical settings to ensure the model's reliability and generalizability.

Overall, our work serves as a foundation for ongoing research aimed at advancing the state-of-the-art in medical image analysis and improving patient outcomes through cutting-edge technology and innovation.

ACKNOWLEDGMENT

I would like to express my sincere gratitude to my supervisor, Dr. Lu Zhenyu, for his invaluable guidance, unwavering support, and mentorship throughout this research endeavour. His expertise, encouragement, and constructive feedback have been instrumental in shaping the direction of this study and pushing me to achieve my best.

I am deeply grateful to my senior colleague, Zhongfeng Chen, for his generous assistance, insightful discussions, and technical expertise.

REFERENCES

[1] A. Saood and I. Hatem, "COVID-19 lung CT image segmentation using deep learning methods: U-Net versus SegNet," *BMC Med Imaging*, vol. 21, no. 1, p. 19, Dec. 2021, doi: 10.1186/s12880-020-00529-5.

[2] A. R. Xavier Annie, "Lung Nodule Segmentation and Classification using U-Net and Efficient-Net," 2023. [Online]. Available: www.ijacsa.thesai.org

[3] R. Rudiansyah, L. Indra Kesuma, and M. Ikhsan Anggara, "Implementation of Image Quality Improvement Methods and Lung Segmentation on Chest X-Ray Images Using U-Net Architectural Modifications," *Computer Engineering and Applications*, vol. 12, no. 2, 2023, [Online]. Available: https://www.kaggle.com/nikhilpandey360/chest-

[4] S. Arvind, J. V. Tembhurne, T. Diwan, and P. Sahare, "Improvised light weight deep CNN based U-Net for the semantic segmentation of lungs from chest X-rays," *Results in Engineering*, vol. 17, p. 100929, Mar. 2023, doi: 10.1016/j.rineng.2023.100929.

[5] W. Nimalsiri, M. Hennayake, K. Rathnayake, T. D. Ambegoda, and D. Meedeniya, "CXLSeg Dataset: Chest X-ray with Lung Segmentation," in *2023 International Conference On Cyber Management And Engineering (CyMaEn)*, IEEE, Jan. 2023, pp. 327–331. doi: 10.1109/CyMaEn57228.2023.10050951.

[6] O. Ronneberger, P. Fischer, and T. Brox, "U-Net: Convolutional Networks for Biomedical Image Segmentation," 2015, pp. 234–241. doi: 10.1007/978-3-319-24574-4_28.

[7] H. Yu, J. Li, L. Zhang, Y. Cao, X. Yu, and J. Sun, "Design of lung nodules segmentation and recognition algorithm based on deep learning," *BMC Bioinformatics*, vol. 22, no. S5, p. 314, Nov. 2021, doi: 10.1186/s12859-021-04234-0.

[8] K. Simonyan and A. Zisserman, "Very deep convolutional networks for large-scale image recognition," *3rd International Conference on Learning Representations, ICLR 2015 - Conference Track Proceedings*, 2015.

[9] E. D. Cubuk, B. Zoph, D. Mane, V. Vasudevan, and Q. V. Le, "AutoAugment: Learning Augmentation Strategies From Data," in *2019 IEEE/CVF Conference on Computer Vision and Pattern Recognition (CVPR)*, IEEE, Jun. 2019, pp. 113–123. doi: 10.1109/CVPR.2019.00020.

[10] M. D. Zeiler, "ADADELTA: An Adaptive Learning Rate Method," Dec. 2012, Accessed: Mar. 06, 2024. [Online]. Available: https://arxiv.org/abs/1212.5701v1

[11] A. Krizhevsky, I. Sutskever, and G. E. Hinton, "ImageNet Classification with Deep Convolutional Neural Networks," in *Advances in Neural Information Processing Systems*, F. Pereira, C. J. Burges, L. Bottou, and K. Q. Weinberger, Eds., Curran Associates, Inc., 2012. [Online]. Available: https://proceedings.neurips.cc/paper_files/paper/2012/file/c399862d3b9d6b76c8436e924a68c45b-Paper.pdf

[12] R. Younisse, R. Ghnemat, and J. Al Saraireh, "Fine-tuning U-net for medical image segmentation based on activation function, optimizer and pooling layer," *International Journal of Electrical and Computer Engineering (IJECE)*, vol. 13, no. 5, p. 5406, Oct. 2023, doi: 10.11591/ijece.v13i5.pp5406-5417.

[13] D. P. Kingma and J. L. Ba, "Adam: A Method for Stochastic Optimization," *3rd International Conference on Learning Representations, ICLR 2015 - Conference Track Proceedings*, Dec. 2014, Accessed: Mar. 05, 2024. [Online]. Available: https://arxiv.org/abs/1412.6980v9

[14] C. H. Sudre, W. Li, T. Vercauteren, S. Ourselin, and M. Jorge Cardoso, "Generalised Dice Overlap as a Deep Learning Loss Function for Highly Unbalanced Segmentations," 2017, pp. 240–248. doi: 10.1007/978-3-319-67558-9_28.

[15] J. Bergstra and Y. Bengio, "Random Search for Hyper-Parameter Optimization," *Journal of Machine Learning Research*, vol. 13, no. 10, pp. 281–305, 2012, [Online]. Available: http://jmlr.org/papers/v13/bergstra12a.html

[16] "Lung segmentation with NASNet-Large-Decoder Net," *arXiv.org*, vol. abs/2303.10315, Mar. 2023, doi: 10.48550/ARXIV.2303.10315.

[17] J. Hou, C. Yan, R. Li, Q. Huang, X. Fan, and F. Lin, "Lung Nodule Segmentation Algorithm With SMR-UNet," *IEEE Access*, vol. 11, pp. 34319–34331, 2023, doi: 10.1109/ACCESS.2023.3264789.

[18] D. Yang, J. Du, K. Liu, Y. Sui, J. Wang, and X. Gai, "Construction of U-Net++ pulmonary nodule intelligent analysis model based on feature weighted aggregation," *Technology and Health Care*, vol. 31, pp. 477–486, Apr. 2023, doi: 10.3233/THC-236041.

[19] M. Y. Kamil and S. A. Hashem, "Segmentation of Chest X-Ray Images Using U-Net Model," *MENDEL*, vol. 28, no. 2, pp. 49–53, Dec. 2022, doi: 10.13164/mendel.2022.2.049.

